

A TRIPLE-ENERGY-SOURCE MODEL FOR SUPERLUMINOUS SUPERNOVA IPTF13EHE

S. Q. WANG^{1,2}, L. D. LIU^{1,2}, Z. G. DAI^{1,2}, L. J. WANG³, AND X. F. WU^{4,5,6}

¹School of Astronomy and Space Science, Nanjing University, Nanjing 210093, China; dzg@nju.edu.cn

²Key Laboratory of Modern Astronomy and Astrophysics (Nanjing University), Ministry of Education, China

³Key Laboratory of Space Astronomy and Technology, National Astronomical Observatories, Chinese Academy of Sciences, Beijing 100012, China

⁴Purple Mountain Observatory, Chinese Academy of Sciences, Nanjing, 210008, China

⁵Chinese Center for Antarctic Astronomy, Chinese Academy of Sciences, Nanjing, 210008, China and

⁶Joint Center for Particle Nuclear Physics and Cosmology of Purple Mountain Observatory-Nanjing University, Chinese Academy of Sciences, Nanjing 210008, China

Draft version July 23, 2018

ABSTRACT

Almost all superluminous supernovae (SLSNe) whose peak magnitudes are $\lesssim -21$ mag can be explained by the ^{56}Ni -powered model, magnetar-powered (highly magnetized pulsar) model or ejecta-circumstellar medium (CSM) interaction model. Recently, iPTF13ehe challenges these energy-source models, because the spectral analysis shows that $\sim 2.5M_{\odot}$ of ^{56}Ni have been synthesized but are inadequate to power the peak bolometric emission of iPTF13ehe, while the rebrightening of the late-time light-curve (LC) and the $\text{H}\alpha$ emission lines indicate that the ejecta-CSM interaction must play a key role in powering the late-time LC. Here we propose a triple-energy-source model, in which a magnetar together with some amount ($\lesssim 2.5M_{\odot}$) of ^{56}Ni may power the early LC of iPTF13ehe while the late-time rebrightening can be quantitatively explained by an ejecta-CSM interaction. Furthermore, we suggest that iPTF13ehe is a genuine core-collapse supernova rather than a pulsational pair-instability supernova candidate. Further studies on similar SLSNe in the future would eventually shed light on their explosion and energy-source mechanisms.

Subject headings: stars: magnetars – supernovae: general – supernovae: individual (iPTF13ehe)

1. INTRODUCTION

Supernovae (SNe) are exceptionally brilliant stellar explosions in the Universe. Over the last decade, dozens of superluminous SNe (SLSNe) whose peak magnitudes are $\lesssim -21$ mag (Gal-Yam 2012) have attracted intense interest from both observational and theoretical astronomers. SLSNe are the rarest class of supernovae discovered so far and have been classified into types I (hydrogen-poor) and II (hydrogen-rich). Comparing the results of Cooke et al. (2012), Quimby et al. (2013), and Taylor et al. (2014), the ratio of the explosion rates of SLSNe to core-collapse SNe (CCSNe) is $\sim (1 - 4) \times 10^{-3}$.

Discriminating among the energy-sources powering the SLSNe is rather tricky. However, these energy sources should leave their imprints on the light curves (LCs) and the spectra of these SLSNe. Only very few SLSNe (e.g., SN 2007bi) can be regarded as the “pair instability SNe (PISNe)” (Barkat et al. 1967; Rakavy & Shaviv 1967; Heger & Woosley 2002; Heger et al. 2003) and explained by the ^{56}Ni -powered model (Gal-Yam et al. 2009)¹, while the majority of SLSNe cannot be solely powered by ^{56}Ni (Quimby et al. 2011; Inserra et al. 2013) but can be explained by the ejecta-circumstellar medium (CSM) interaction model (Chevalier & Irwin 2011; Ginzburg & Balberg 2012) or magnetar-powered (ultra-highly magnetized pulsar) model (Kasen & Bildsten 2010; Woosley 2010; Dessart et al. 2012; Inserra et al. 2013; Wang et al.

2015a). Because of the absence of emission lines indicative of the ejecta-CSM interaction, the magnetar model is preferred in explaining almost all SLSNe-I (e.g. Inserra et al. 2013; Nicholl et al. 2013; Howell et al. 2013; McCrum et al. 2014; Vreeswijk et al. 2014; Nicholl et al. 2014; Wang et al. 2015a; Metzger et al. 2015; Dai et al. 2016; Kasen et al. 2016; Wang et al. 2016). Meanwhile, the ejecta-CSM interaction model works well in explaining SLSNe-II, especially superluminous SNe II_n (Smith & McCray 2007; Moriya et al. 2013a).

In principle, ^{56}Ni should be taken into account in light-curve modeling for all SLSNe. From the photometric aspect, however, SLSNe’s ^{56}Ni yields are usually rather small (e.g. Inserra et al. 2013) and the luminosities provided by ^{56}Ni are outshone by magnetars or ejecta-CSM interaction, except for some PISN candidates that might be mainly powered by ^{56}Ni . Besides, ^{56}Ni yields are difficult to be determined precisely owing to the lack of late-time spectra for most SNe. Hence, excluding a few PISN candidates, previous modelings for most LCs of SLSNe-I omitted the contributions of ^{56}Ni .

There are some more complicated cases: for some SLSNe-II, e.g. SN 2006gy, adding several M_{\odot} of ^{56}Ni can make the fitting more reliable, the “ ^{56}Ni +interaction” model has been employed (Agnoletto et al. 2009; Chatzopoulos et al. 2012, 2013). No SLSN has involved with all three energy sources so far; Wang et al. (2015b) suggested that some luminous SNe Ic with peak magnitudes ~ -20 mag must be explained by a unified scenario containing the contributions from ^{56}Ni and a magnetar (“ ^{56}Ni +interaction” model) since they cannot be

¹ However, Dessart et al. (2012) and Nicholl et al. (2013) disfavored the ^{56}Ni -powered model in explaining SN 2007bi and other similar events.

powered solely by ^{56}Ni (see also Greiner et al. 2015) but the contribution from ^{56}Ni cannot be neglected (see also Bersten et al. 1967).

Recently, an SLSN-I at redshift $z = 0.3434$, iPTF13ehe, might change the conclusions above. Yan et al. (2015) analyzed the light curve and spectra of iPTF13ehe and found that the peak bolometric luminosity of iPTF13ehe is $\sim 1.3 \times 10^{44}$ erg s $^{-1}$. If this SLSN was powered by ^{56}Ni , more than $(13 - 16)M_{\odot}$ of ^{56}Ni must be synthesized to power the peak bolometric emission (Yan et al. 2015). However, the late-time spectral analysis indicated that the mass of ^{56}Ni synthesized is $\sim 2.5 M_{\odot}$. This amount of ^{56}Ni , although it cannot be ignored, is inadequate to power the peak bolometric luminosity. Therefore, Yan et al. (2015) argued that the early LC must be powered by multiple power sources.

Furthermore, the presence of H α emission lines in the late-time spectrum and the rebrightening in the late-time LC show an unambiguous signature for interactions between the SN ejecta and a hydrogen-rich CSM. Hence, any model with single power source or double power sources is challenged in explaining the LC of iPTF13ehe. A triple-power-source model should be seriously considered.

In this paper, we propose a triple-energy-source model for iPTF13ehe and try to understand its explosion mechanism and LC. This paper is organized as follows. In Sections 2 and 3, we fit the early-time and late-time LC using double and triple energy-source models, respectively. In Sections 4 and 5, we discuss and conclude our results.

2. MODELING THE EARLY-TIME LC

We start by studying the early LC and determining the power sources of iPTF13ehe. As pointed out by Yan et al. (2015), $\sim 2.5M_{\odot}$ of ^{56}Ni were synthesized while $\gtrsim 13-16M_{\odot}$ of ^{56}Ni are required to account for the LC peak. Therefore, there should be other energy sources to aid the high peak-luminosity of iPTF13ehe. The early-time spectra shows no H emission lines, indicating that the ejecta-CSM interaction can be neglected in the early-time luminosity evolution. Hence, the energy source aiding the SN might be a magnetar spin-down input. The possibility that iPTF13ehe is a CCSN and can be aided by a magnetar was also pointed out by Yan et al. (2015), although they didn't provide further analysis. Considering the contribution from ^{56}Ni that cannot be neglected, the most reasonable model should contain contributions from both ^{56}Ni and a magnetar. Wang et al. (2015b) have constructed such a unified model for SNe Ic and explained three luminous SNe Ic. We here employ this model to fit the LC of iPTF13ehe.

Supposing that the ratio of the r -band flux to bolometric flux remains nearly constant around the peak and in the late-time, we scale the r -band luminosities to obtain the bolometric luminosities. The scaled bolometric luminosities are rough, but they can be regarded as an approximation of real values. These data are plotted in Fig. 1. In this section, we use some models to fit the early-time LC. The photospheric velocity and the optical opacity κ are fixed to $\sim 13,000$ km s $^{-1}$ (Yan et al. 2015) and 0.2 cm $^{-2}$ g $^{-1}$, respectively.

2.1. ^{56}Ni Model

The first of the models employed here is the ^{56}Ni -powered model. We find that when the ejecta mass $M_{\text{ej}} = 35 M_{\odot}$, the gamma-ray opacity $\kappa_{\gamma} \simeq 0.018$ cm $^{-2}$ g $^{-1}$, and the ^{56}Ni mass $M_{\text{Ni}} \sim 19 M_{\odot}$, the theoretical LC can match the observational data at early times ($t \lesssim 137$ days), as can be seen in Fig. 1 (the dash-dotted line). The ^{56}Ni mass obtained here is slightly larger than the value $\sim (13 - 16)M_{\odot}$ inferred by Yan et al. (2015).

However, the ratio of M_{Ni} ($\sim 19 M_{\odot}$) to M_{ej} ($35 M_{\odot}$) is $\sim 50\%$, significantly exceeding the upper limit of the values for CCSNe (the ratio of ^{56}Ni mass to the ejecta mass is $\lesssim 20\%$ (Umeda & Nomoto 2008)). Therefore, the ^{56}Ni -powered model can be excluded in explaining the data.

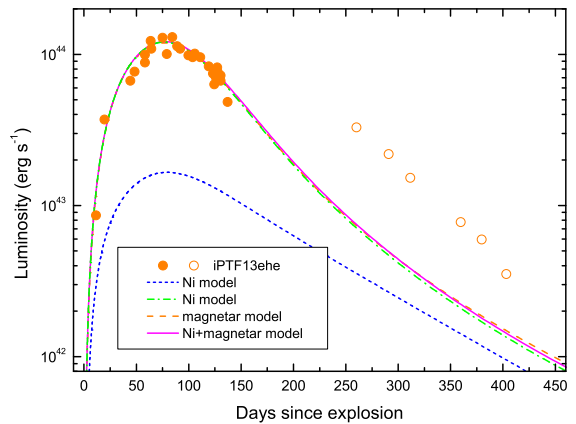


FIG. 1.— Modeling iPTF13ehe’s early-time LC using ^{56}Ni , magnetar, and hybrid (^{56}Ni + magnetar) models. Data are obtained from Yan et al. (2015). The early-time and late-time bolometric luminosities scaled from r -band ones are shown as the orange filled circles and orange unfilled circles, respectively. The dash-dotted line is the LC powered by $19 M_{\odot}$ of ^{56}Ni ; the dashed line is the LC powered by a magnetar; the solid line is the LC powered by ^{56}Ni and a magnetar. The short dashed line is the LC powered by $2.5 M_{\odot}$ of ^{56}Ni with full trapping of gamma-rays. The other model parameter values are shown in the text.

2.2. Magnetar Model and Magnetar+ ^{56}Ni Model

In the magnetar-powered model, if the initial rotational period of the magnetar $P_0 = 2.45$ ms, the surface magnetic field $B = 8 \times 10^{13}$ G, $\kappa_{\gamma} \simeq 0.018$ cm $^{-2}$ g $^{-1}$, then the dashed line in Fig. 1 is plotted to obtain an equivalently good fitting. Since the spectral analysis has inferred that the SN explosion produced $\sim 2.5 M_{\odot}$ of ^{56}Ni , we take into account the contribution from ^{56}Ni and use the hybrid model, in which the initial period of the magnetar P_0 is larger slightly, ~ 2.55 ms. From the fit, we can get other two important physical quantities relevant to the next section, i.e., the rise time $t_r \sim 81$ days and the kinetic energy of the SN explosion, $E_{\text{SN}} = (3/10)M_{\text{ej}}v^2 \sim 3.5 \times 10^{52}$ erg.

2.3. Further Analysis for the Parameters of iPTF13ehe

A caveat on the degeneracy of model parameters should be clarified here. The effective light-curve

timescale $\tau_m = (2\kappa M_{\text{ej}}/\xi v c)^{1/2}$ (Arnett 1982) determines the width and therefore the rise time of the LCs of SNe, where c is the speed of light and $\xi = 4\pi^3/9 \simeq 13.8$ is a constant. If the value of $\kappa M_{\text{ej}}/v$ is invariant, LCs around the peak are the same. Although the photospheric velocity v of iPTF13ehe is fixed to 13,000 km s^{-1} , the degeneracy of κ and M_{ej} is still difficult to be broken, because larger κ requires smaller M_{ej} for the same level of fittings. The optical opacity of H- and He-deficient ejecta has been assumed to be 0.06 $\text{cm}^2 \text{g}^{-1}$ (e.g., Valenti et al. 2011; Lyman et al. 2016), 0.07 $\text{cm}^2 \text{g}^{-1}$ (e.g., Taddia et al. 2015; Wang et al. 2015b), 0.08 $\text{cm}^2 \text{g}^{-1}$ (e.g., Arnett 1982; Mazzali et al. 2000), 0.10 $\text{cm}^2 \text{g}^{-1}$ (e.g., Nugent et al. 2011; Inserra et al. 2013; Wheeler et al. 2015), and 0.2 $\text{cm}^2 \text{g}^{-1}$ (e.g., Kasen & Bildsten 2010; Nicholl et al. 2014). We assume that $\kappa = 0.2 \text{ cm}^2 \text{g}^{-1}$ throughout this paper and get the ejecta mass $M_{\text{ej}} \sim 35M_{\odot}$. If we assume a smaller κ , e.g., $\kappa = 0.1 \text{ cm}^2 \text{g}^{-1}$, then the ejecta mass becomes larger, $M_{\text{ej}} \sim 70M_{\odot}$. The latter is consistent with the lower limit derived by Yan et al. (2015). Provided that iPTF13ehe is a genuine core-collapse SN, the ejecta with mass of $35M_{\odot}$ is preferred.

3. MODELING THE LATE-TIME LC

We have demonstrated that the hybrid model containing the contributions from a magnetar and ^{56}Ni can well fit the early-time LC of iPTF13ehe, but the late-time rebrightening cannot be explained by such a hybrid model. Yan et al. (2015) found that the late-time spectrum of the SN displayed H α emission lines which are usually present in SNe II and inferred that a Hydrogen shell ejected about 40 years before the SN explosion, locating at a distance of $\sim 4 \times 10^{16}$ cm from the SN progenitor. When the SN ejecta run into the shell, an interaction was triggered and thus the r -band LC was rebrightened and the H α emission was prompted. Therefore, both the photometric and spectral features indicate that the interaction between the ejecta and CSM must play an important role in powering the late-time LC (Yan et al. 2015).

However, the exact time of the emergence of the ejecta-CSM interaction is uncertain due to the lack of the photometric data at $\sim 60 - 170$ days and the spectral data at 13 – 251 days after the peak. Nevertheless, the fact that there is no rebrightening in ~ 56 days after the peak provides a lower limit on the interaction onset time, while the rebrightening at ~ 180 days after the peak offers an upper limit. Therefore, we suppose that the rebrightening started at $\sim 56 - 180$ days after the peak. Adopting $t_{\text{r}} \sim 81$ days, we conclude that the interaction should be triggered between $\sim 137 - 261$ days after the SN explosion. Hence, it is reasonable to suppose that the onset time of interaction between the ejecta and the CSM-shell t_i is ~ 140 days.

According to Equations (14)-(16) and (20) of Chatzopoulos et al. (2012), we reproduce the late-time LC powered by the ejecta-CSM interaction, seen in Fig. 2. The fit parameters are the optical opacity of the H-shell $\kappa' = 0.34 \text{ cm}^2 \text{g}^{-1}$, the ejecta mass $M_{\text{ej}} = 35M_{\odot}$, the SN kinetic energy $E_{\text{SN}} = 3.5 \times 10^{52}$ erg (these two parameters are derived from the previous section), the slope of the inner density profile of the ejecta $\delta = 0$, the

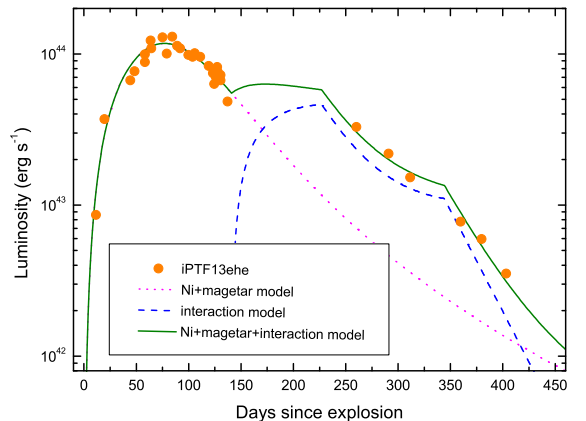


FIG. 2.— Modeling iPTF13ehe’s whole LC by using the triple-energy-source (^{56}Ni + magnetar + interaction) model. Data are obtained from Yan et al. (2015). The bolometric luminosities scaled from r -band ones are shown as the orange filled circles. The dotted line is the LC powered by ^{56}Ni and a magnetar; the dashed line is the LC powered by the ejecta-CSM interaction; the solid line is the LC powered by the triple-energy-source (“ ^{56}Ni +magnetar+ejecta-CSM interaction”) model. The values of other parameters are shown in the text.

slope of the outer density profile of the ejecta $n = 7$, the power-law exponent for the CSM density profile $s = 0$ (corresponding to a uniform-density shell), the density of the CSM $\rho_{\text{CSM}} = 10^{-14} \text{ g cm}^{-3}$, the mass of the CSM $M_{\text{CSM}} = 27M_{\odot}$, the onset time of interaction between the ejecta and the CSM-shell $t_i \sim 140$ days, the conversion efficiency from kinetic energy to radiation $\epsilon = 0.05$ that is comparable to the typical value $\epsilon \sim 0.1$ (Moriya et al. 2013b).

The density of the CSM shell in our model is one order of magnitude larger than the value derived by Yan et al. (2015). Since the shock-ionized CSM shell is probably optically thin to the Thomson scattering (Yan et al. 2015), $\tau_{\text{Thomson}} = \kappa' \rho w \leq 1$, where w is the width of the shell, $\kappa' (M_{\text{CSM}}/4\pi R^2 w) w = \kappa' (M_{\text{CSM}}/4\pi R^2) \leq 1$, so $M_{\text{CSM}} \leq 4\pi R^2/\kappa'$. Yan et al. (2015) supposed that the interaction time is 251 days after the peak, and derived that $R \simeq 4 \times 10^{16}$ cm. If $w = 0.1R$, and $\kappa' = 0.34 \text{ cm}^2 \text{g}^{-1}$, then $M_{\text{CSM}} \leq 30M_{\odot}$, $n = \rho/m_{\text{H}} \leq 1/\kappa' w m_{\text{H}} \sim 4 \times 10^8 \text{ cm}^{-3}$ (Yan et al. 2015), and $\rho \leq 0.74 \times 10^{-15} \text{ g cm}^{-3}$.

This difference is partly caused by the uncertainty of the onset time of the ejecta-CSM interaction. We suppose that the interaction time is ~ 60 days after the peak and then have $R = vt \sim 1.6 \times 10^{16}$ cm; if $w = 0.1R$, and $\kappa' = 0.34 \text{ cm}^2 \text{g}^{-1}$, then $M_{\text{CSM}} \leq 5M_{\odot}$, $n \leq 1.1 \times 10^9 \text{ cm}^{-3}$, and $\rho \leq 1.84 \times 10^{-15} \text{ g cm}^{-3}$. As pointed out by Yan et al. (2015), the possibility that the CSM shell might be partly ionized rather than fully ionized cannot be excluded. If the ratio of ionized CSM to total CSM is $\sim 1/5.4$, then $\rho_{\text{CSM}} \sim 10^{-14} \text{ g cm}^{-3}$, and $M_{\text{CSM}} \sim 27M_{\odot}$, being consistent with the values of our fitting parameters.

As shown in Fig. 2, the LC powered by the triple power-source model (“ ^{56}Ni +magnetar+ejecta-CSM interaction”) model is well consistent with the data. If

we ignore the contribution from ^{56}Ni , the LC can be reproduced by the magnetar and ejecta-CSM interaction.

We caution that the bolometric LC is obtained by scaling the r -band LC and therefore is not accurate enough. The uncertainties in the bolometric luminosities prevent us from getting precise estimate of the model parameters. Nevertheless, this does not change the facts that the early-time LC is mainly powered by a magnetar rather than ^{56}Ni and that the late-time LC requires adding the ejecta-CSM interaction. More accurate bolometric corrections can pose more stringent constraints on the parameters.

4. DISCUSSIONS

The ^{56}Ni production is usually ineffective after the explosion of a neutrino-driven CCSN. Radioactive ^{56}Ni in a neutrino-driven CCSN is mainly synthesized in two ways: a neutrino-driven wind and an explosive nuclear burning of silicon (and other intermediate-mass elements) heated to a temperature exceeding 5×10^9 K. The neutrino-driven wind can produce $\sim 10^{-3}M_{\odot}$ of ^{56}Ni and can be neglected; the amount of ^{56}Ni synthesized in shock-heating silicon shell is related with the shock energy and therefore the kinetic energy of a CCSN. When the kinetic energy is $\sim 10^{51}$ erg, the mass of ^{56}Ni is $\sim (0.05 - 0.1)M_{\odot}$. If the neutron star left behind the explosion is a millisecond magnetar, it can help the ejecta synthesize additional ^{56}Ni up to $\sim 0.2M_{\odot}$ (Suwa & Tominaga 2015). The total amount of ^{56}Ni from these processes is $\lesssim 0.3M_{\odot}$, significantly less than $2.5 M_{\odot}$.

Therefore, it seems that the model containing the contributions from $2.5 M_{\odot}$ of ^{56}Ni and a magnetar is problematic. However, the possibility that the ^{56}Ni mass of iPTF13ehe has been overestimated cannot be completely excluded. We can get some indirect clues from SN 2007bi: Gal-Yam et al. (2009) proposed that the amount of ^{56}Ni synthesized by SN 2007bi is $\sim 5M_{\odot}$ by matching the low-quality nebular-phase spectrum and concluded that SN 2007bi is a PISN, while Dessart et al. (2012) showed that the PISN model must produce cool photospheres, red spectra and narrow-line profiles which conflict with observational properties of SN 2007bi, and concluded that SN 2007bi might be powered by a magnetar. This example indicates that the simple spectral analysis is not enough to determine the precise value of ^{56}Ni yield and a more detailed analysis is needed. In this paper, we can regard $\sim 2.5M_{\odot}$ as the upper limit of ^{56}Ni yield of iPTF13ehe.

We note that SN ejecta-CSM interaction might also be a promising scenario for explaining the early-time LC of iPTF13ehe. If the progenitor experiences some eruptions and expels some discrete shells before its explosion, the ejecta can collide these shells at different epochs and the interactions between the ejecta and these shells can power the early-time LC. The intermittent spectral observations at early times might miss the spectral features. In this scenario, the putative millisecond magnetar can be removed and the central remnant is therefore a black hole. However, how does the explosion synthesize $\sim 2.5M_{\odot}$ of ^{56}Ni in this scenario remains an open problem.

5. CONCLUSIONS

We have analyzed and fitted the LC for iPTF13ehe which is an SLSN I with peak bolometric luminosity $\sim 1.3 \times 10^{44}$ erg s^{-1} . Using the ^{56}Ni -powered model, we found that $\sim 19M_{\odot}$ of ^{56}Ni are required, confirming the conclusion reached by Yan et al. (2015). Spectral analysis performed by Yan et al. (2015) shows that the SLSN synthesized $\sim 2.5M_{\odot}$ of ^{56}Ni but this amount of ^{56}Ni is inadequate to power the peak luminosity.

We proposed that the most reasonable model accounting for the early-time LC is the magnetar-dominated model containing the contributions from a magnetar with $P_0 = 2.45 - 2.55$ ms and $B = 8 \times 10^{13}$ G and $\lesssim 2.5M_{\odot}$ of ^{56}Ni . The LCs reproduced by this model are in good agreement with early-time observations of iPTF13ehe. The energy released by the magnetar is dominant in powering the optical LC of iPTF13ehe.

While proposing this hybrid model containing triple energy-sources, we also note that this model is not unique model of explaining iPTF13ehe since the early LC might also be powered by the ejecta-CSM interaction and ^{56}Ni . Since the CCSNe usually produce $\lesssim 0.3M_{\odot}$ of ^{56}Ni , $\sim 2.5M_{\odot}$ of ^{56}Ni is problematic in both “magnetar+ ^{56}Ni ” model and “interaction+ ^{56}Ni ”. We regard $\sim 2.5M_{\odot}$ as the upper limit and call for more detailed analysis.

An important spectral feature owned by iPTF13ehe is $H\alpha$ emission lines in its late-time spectrum. These lines, together with the rebrightening of the late-time LC (Yan et al. 2015), indicate that the interaction between the SN ejecta and the CSM has been triggered. The hybrid model involving ^{56}Ni and magnetar cannot account for the late-time rebrightening. We find that the ejecta-CSM interaction model can explain the rebrightening and is the natural requirement accounting for the $H\alpha$ emission lines. Therefore, we use the model containing a magnetar, ^{56}Ni , and ejecta-CSM interaction to fit the whole LC.

Finally, we discuss the explosion nature of iPTF13ehe. The physical properties of the progenitors, the explosion mechanisms and energy-source mechanisms of SLSNe are still ambiguous and controversial (see Dessart et al. 2012; Nicholl et al. 2013, for further analysis). As emphasized by Yan et al. (2015), the massive Hydrogen-rich shell must have been expelled by the “pulsational pair-instability (PPI)” mechanism (Heger et al. 2003; Woosley et al. 2007; Pastorello et al. 2008; Chugai 2009; Chatzopoulos & Wheeler 2012). The ejecta colliding with CSM shell contains $\lesssim 2.5M_{\odot}$ of ^{56}Ni and $\gtrsim 3.5 \times 10^{52}$ erg of kinetic energy. This ejecta is not a shell following the hydrogen-rich shell, because Heger et al. (2003) pointed out that the shell expelled by PPI contains no ^{56}Ni and its kinetic energy is up to several times 10^{51} erg. The kinetic energy of the ejecta of iPTF13ehe is at least one order of magnitude higher than that of each PPI pulsed shell. Therefore, we propose that iPTF13ehe itself is a genuine CCSN rather than a PPISN candidate, while the hydrogen-rich massive shell could be caused by a PPI pulse ~ 20 years before the CCSN explosion ($\delta t \sim vt_i/v_{\text{CSM}} \sim 13,000$ km/s \times 140 days/300 km/s ~ 17 years, the velocity of the CSM shell v_{CSM} was inferred by Yan et al. (2015)).

Yan et al. (2015) estimated that at least 15% of SLSNe-I may own such interaction features for late-time spectra. We expect that future studies focusing on sim-

ilar SLSNe should provide further insight into their explosion and energy-source mechanisms.

We thank an anonymous referee for valuable comments and constructive suggestions that have improved our manuscript. This work was supported by the National Basic Research Program (“973” Program) of China

(grant No. 2014CB845800) and the National Natural Science Foundation of China (grant Nos. 11573014 and 11322328). X.F.W. is partially supported by the Youth Innovation Promotion Association (2011231), and the Strategic Priority Research Program “The Emergence of Cosmological Structures” (grant No. XDB09000000) of the Chinese Academy of Sciences.

REFERENCES

- Agnoletto., I, Benetti, S., Cappellaro, E., et al. ApJ, 2009, 691, 1348
- Arnett, W. D. 1982, ApJ, 253, 785
- Barkat, Z., Rakavy, G., & Sack, N. 1967, Phys. Rev. Lett., 18, 379
- Bersten, M. C., Benvenuto, O. G., Orellana, M., & Nomoto, K. 2016, ApJL, 817, L8
- Chatzopoulos, E., & Wheeler, J. C. 2012, ApJ, 760, 154
- Chatzopoulos, E., Wheeler, J. C., & Vinko, J. 2012, ApJ, 746, 121
- Chatzopoulos, E., Wheeler, J. C., Vinko, J., Horvath, Z. L., & Nagy, A. 2013, ApJ, 773, 76
- Chevalier, R. A., & Irwin, C. M. 2011, ApJL, 729, L6
- Chugai, N. N. 2009, MNRAS, 400, 866
- Cooke, J., Sullivan, M., Gal-Yam, A., et al. 2012, Nature, 491, 228
- Dai, Z. G., Wang, S. Q., Wang, J. S., Wang, L. J., & Yu, Y. W. 2016, ApJ, 817, 132
- Dessart, L., Hillier, D. J., Waldman, R., Livne, E., & Blondin, S. 2012, MNRAS, 426, L76
- Gal-Yam, A., Mazzali, P., Ofek, E. O., et al. 2009, Nature, 462, 624
- Gal-Yam, A. 2012, Science, 337, 927
- Ginzburg, S., & Balberg, S. 2012, ApJ, 757, 178
- Greiner, J., Mazzali, P. A., Kann, D. A., et al. 2015, Nature, 523, 189
- Heger, A., & Woosley, S. E. 2002, ApJ, 567, 532
- Heger, A., Fryer, C. L., Woosley, S. E., Langer, N. & Hartmann, D. H. 2003, ApJ, 591, 288
- Howell, D. A., Kasen, D., Lidman, C., et al. 2013, ApJ, 779, 98
- Insera, C., Smartt, S. J., Jerkstrand, A., et al. 2013, ApJ, 770, 128
- Kasen, D., & Bildsten, L. 2010, ApJ, 717, 245
- Kasen, D., Metzger, B. D., & Bildsten, L. 2016, ApJ, 821, 36
- Lyman, J. D., Bersier, D., James, P. A., Mazzali, P. A., Eldridge, J., Fraser, M., & Pian, E. 2016, MNRAS, 457, 328
- Mazzali, P. A., Iwamoto, K., & Nomoto, K. 2000, ApJ, 545, 407
- McCrum, M., Smartt, S. J., Kotak, R., et al. 2014, MNRAS, 437, 656
- Metzger, B. D., Margalit, B., Kasen, D., & Quataert, E. 2015, MNRAS, 454, 3311
- Moriya, T. J., Blinnikov, S. I., Tominaga, N., Yoshida, N., Tanaka, M., Maeda, K., & Nomoto, K. 2013a, MNRAS, 428, 1020
- Moriya, T. J., Maeda, K., Taddia, F., Sollerman, J., Blinnikov, S. I., & Sorokina, E. I. 2013b, MNRAS, 435, 1520
- Nicholl, M., Smartt, S. J., Jerkstrand, A., et al. 2013, Nature, 502, 346
- Nicholl, M., Jerkstrand, A., Inserra, C., et al. 2014, MNRAS, 444, 2096
- Nugent, P. E., Sullivan, M., Cenko, S. B., et al. 2011, Nature, 480, 344
- Pastorello, A., Mattila, S., Zampieri, L., et al. 2008, MNRAS, 389, 113
- Quimby, R. M., Kulkarni, S. R., Kasliwal, M. M., et al. 2011, Nature, 474, 487
- Quimby, R. M., Yuan, F., Akerlof, C., et al. 2013, MNRAS, 2013, 431, 912
- Rakavy, G., & Shaviv, G. 1967, ApJ, 148, 803
- Smith, N., & McCray, R. 2007, ApJL, 671, L17
- Suwa, Y., & Tominaga, N. 2015, MNRAS, 451, 282
- Taddia, F., Sollerman, J., Leloudas, G., Stritzinger, M. D., Valenti, S., Galbany, L., Kessler, R., Schneider, D. P., & Wheeler, J. C. 2015, A&A, 574, 60
- Taylor, M., Cinabro, D., Dilday, B., et al. 2014, ApJ, 792, 135
- Umeda, H., & Nomoto, K. 2008, ApJ, 673, 1014
- Valenti, S., Fraser, M., Benetti, S., et al. 2011, MNRAS, 416, 3138
- Vreeswijk, P. M., Savaglio, S., Gal-Yam, A., et al. 2014, ApJ, 797, 24
- Wang, L. J., Wang, S. Q., Dai, Z. G., Xu, D., Han, Y. H., Wu, X. F., & Wei, J. Y. 2016, ApJ, 821, 22
- Wang, S. Q., Wang, L. J., Dai, Z. G., & Wu, X. F. 2015a, ApJ, 799, 107
- Wang, S. Q., Wang, L. J., Dai, Z. G., & Wu, X. F. 2015b, ApJ, 807, 147
- Wheeler, J. C., Johnson, V., & Clocchiatti, A. 2015, MNRAS, 450, 1295
- Woosley, S. E. 2010, ApJL, 719, L204
- Woosley, S. E., Blinnikov, S., & Heger, A. 2007, Nature, 450, 390
- Yan, L., Quimby, R., Ofek, E., et al. 2015, ApJ, 814, 108